

Monomeric Bistability and the Role of Autoloops in Gene Regulation

Stefanie Widder
Javier Macía
Ricard V. Solé

SFI WORKING PAPER: 2008-10-044

SFI Working Papers contain accounts of scientific work of the author(s) and do not necessarily represent the views of the Santa Fe Institute. We accept papers intended for publication in peer-reviewed journals or proceedings volumes, but not papers that have already appeared in print. Except for papers by our external faculty, papers must be based on work done at SFI, inspired by an invited visit to or collaboration at SFI, or funded by an SFI grant.

©NOTICE: This working paper is included by permission of the contributing author(s) as a means to ensure timely distribution of the scholarly and technical work on a non-commercial basis. Copyright and all rights therein are maintained by the author(s). It is understood that all persons copying this information will adhere to the terms and constraints invoked by each author's copyright. These works may be reposted only with the explicit permission of the copyright holder.

www.santafe.edu



SANTA FE INSTITUTE

Stefanie Widder,^{1,*} Javier Macía^{†,1,*} and Ricard Solé^{1,2,*}

¹Complex System Lab (ICREA-UPF), Barcelona Biomedical Research Park (PRBB-GRIB), Dr. Aiguader 88, 08003 Barcelona, Spain

²Santa Fe Institute, 1399 Hyde Park Road, Santa Fe NM 87501, USA

(Dated: September 4, 2008)

Genetic toggle switches are widespread in gene regulatory networks (GRN). It is often assumed that negative feedbacks with cooperative binding (i.e. the formation of dimers or multimers) are a prerequisite for bistability. Here we analyze the relation between bistability in GRN under monomeric regulation and the role of autoloops in a deterministic setting. Using a simple geometric argument, we show analytically that bistability can also emerge without multimeric regulation, provided that at least one regulatory autoloop is present.

Bistability is known to pervade key relevant biological phenomena [1] including, e.g. the determination of cell fate in multicellular organisms [2], stem cell switching [3] or cell-cycle regulation [4]. This capacity of achieving multiple internal states is at the core of a plethora of regulatory mechanisms, often associated to small genetic circuits, including switches [5–9] and oscillators [10, 11]. Understanding their logic and how it will change under parameter tuning are two important goals of systems biology. A general consensus indicates that such switches are based on a mutual repression of two transcription factors (figure 1a): protein A inhibits the synthesis of protein B and vice versa [12]. They can be in two different stable states and may change from one to the other spontaneously or due to an external signal [12–15]. Typically, their regulatory proteins are known to form homodimers (or multimers) to be effective transcription factors [6, 16, 17] allowing to turn ON or OFF the state of target genes [12, 18, 19]. For general systems without any specific assumptions, multimeric regulation was assumed to be essential to obtain bistable behaviour [22, 23]. Despite, monomeric bistability has been found in particular, bimolecular systems under the indispensable key-assumptions of Michaelis-Menten kinetics and constancy of the total amount of proteins [21]. Also, some kind of multistability is possible in a stochastic scenario without cooperative binding [13, 20], but under fully symmetric interactions. However, the flips between the two states are also stochastic and the observed alternative states cannot be stabilized (as it occurs in real biological switches) due to the effectively monostable character of the system without noise. In deterministic dynamics, bistability requires the existence of three fixed points. In this paper we demonstrate, to our knowledge for the first time, that deterministic bistability can emerge for two-component gene circuits by considering solely auto-

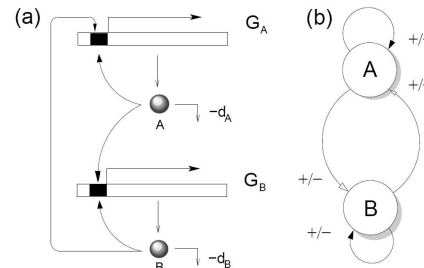


FIG. 1: (a) A genetic circuit with monomeric autoloops and cross-regulation involving two genes (G_A, G_B) coding for two proteins (A, B) acting as transcription factors. Under certain conditions, this type of genetic circuit can show bistability. Here all possible regulatory modes are shown (+/-). (b) Simplified diagram summarizing the logic of this system.

regulatory loops. This is unlike the previously briefly mentioned cases [13, 21], where bistability is not generated by the intrinsic characteristics of the circuits, but by external conditions. Our analysis is based on simple geometrical features associated to the system's nullclines and their crossings. As shown below, the presence of an autoloop introduces essential geometrical constraints responsible for the existence of three fixed points. Our results can help understanding the essential role of autoloops in small natural circuits and their synthetic counterparts.

Genetic circuit. We focus our analysis on the most general system formed by two genes. Gene A is expressed under the constraints of two different monomeric regulatory modes. Protein A exhibits an auto-regulatory loop by binding to its own promoter, as well as a cross-regulation mediated by protein B . Gene B expression is analogously regulated (see figure 1). We consider the general case without any specific assumptions about the type of regulatory interactions, i.e. activation or inhibition, but introduce them as a tunable parameters α . The basic dynamical properties of the circuit can be described by the following set of ODEs obtained from the

[†]To whom correspondence should be addressed. Email: javier.macia@upf.edu

* All authors have contributed equally.

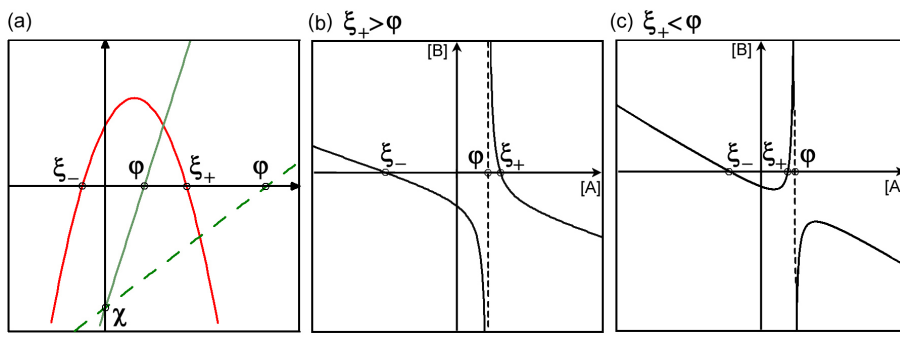


FIG. 2: (a) Graphical representation of the nullcline's components. The numerator is the parabolic curve and the denominator the straight line. Two feasible scenarios are shown: the solid line denotes $\xi_+ > \varphi$, the dashed line corresponds to $\xi_+ < \varphi$. (b),(c) Qualitative behaviour of the nullclines applying the two possible conditions.

set of biochemical reactions:

$$\frac{dA}{dt} = \gamma_A \left(\frac{1 + \omega_l^A \alpha_l^A A + \omega_c^B \alpha_c^B B}{1 + \omega_l^A A + \omega_c^B B} \right) - d_A A \quad (1)$$

$$\frac{dB}{dt} = \gamma_B \left(\frac{1 + \omega_l^B \alpha_l^B B + \omega_c^A \alpha_c^A A}{1 + \omega_l^B B + \omega_c^A A} \right) - d_B B$$

We are assuming basal transcription, the standard rapid equilibrium approximations supposing that binding and unbinding processes are faster than synthesis and degradation, and constancy of the total number of promoter sites. Furthermore, the concentration of the other biochemical elements involved remains constant during time and can be subsumed in the kinetic constant γ_i . The binding equilibrium of the autoloop and the cross-regulators are denoted by ω_l^i and ω_c^i , respectively. Furthermore α_l^i and α_c^i denote the regulatory rates with respect to the basal transcription, for the autoloop and cross-regulation respectively. Values < 1 correspond to inhibitory regulation, whereas > 1 accounts for activation. Finally, d_i is the degradation rate of protein i . For a detailed description of this type of calculus, see [17].

Nullclines analysis. In order to analyze the system's dynamics we obtain the following expressions for the nullclines imposing $\dot{A} = 0$ and $\dot{B} = 0$ considering monomeric regulation:

$$B = \frac{\gamma_A + \gamma_A \omega_l^A \alpha_l^A A - d_A A - d_A \omega_l^A A^2}{\omega_c^B (d_A A - \gamma_A \alpha_c^B)} \quad (2)$$

$$A = \frac{\gamma_B + \gamma_B \omega_l^B \alpha_l^B B - d_B B - d_B \omega_l^B B^2}{\omega_c^A (d_B B - \gamma_B \alpha_c^A)} \quad (3)$$

The number of crossing points between (2) and (3) defines the number of different fixed points within the system. Both nullclines have mathematically symmetric expressions, tunable by the set of parameters. This symmetry facilitates their analysis due to interchangeability of the characteristic features. Hence, the problem can be evaluated by reducing the analysis to one expression. Here (2) is analyzed.

Geometrical features. In order to perform a general analysis of the nullclines we study the single components (numerator and denominator) of the expressions independently, see figure 2(a). The numerator is a parabolic function having two analytically well defined crossing points ($\xi_+ > 0$ and $\xi_- < 0$) with the horizontal axis given by

$$\xi_{\pm} = \frac{-d_A + \alpha_l^A \gamma_A \omega_l^A \pm \sqrt{4d_A \gamma_A \omega_l^A + (d_A - \alpha_l^A \gamma_A \omega_l^A)^2}}{2d_A \omega_l^A} \quad (4)$$

The denominator is a linear function crossing the horizontal axis in $\varphi = \gamma_A \alpha_c^B / d_A$. The points φ and ξ_+ are the upper and lower bound of the protein concentrations of the system within the biological meaningful region. Combining the two components, two different scenarios are feasible, $\varphi < \xi_+$ or $\varphi > \xi_+$, comprising different geometrical features. In both cases we find two crossing points with the horizontal axis in ξ_{\pm} , no inflection points, and the nullclines tending towards their oblique asymptotes with an identical slope $m = -\omega_l^A / \omega_c^B$ for both settings $A \rightarrow \pm\infty$. From this expression we see that the autoloop is related with certain geometrical features. Systems without auto-regulatory loops ($\omega_l^A = 0$) do not exhibit oblique asymptotes, but horizontal. As shown later the existence of oblique asymptotes is closely related with the number of possible fixed points and bistability.

In the first case, $\xi_+ > \varphi$, we obtain a vertical asymptote in φ with its lateral behaviour given by $\lim_{A \rightarrow \varphi^{\pm}} (B)_{\dot{A}=0} = \pm\infty$. For the second case, $\xi_+ < \varphi$, we find similar asymptotes with opposite lateral behaviour according to $\lim_{A \rightarrow \varphi^{\pm}} (B)_{\dot{A}=0} = \mp\infty$. In order to determine possible extrema of the nullcline ($dB/dA = 0$), we find, after some algebra, that the inequality

$$d_A (\alpha_c^B - 1) + \alpha_c^B \gamma_A \omega_l^A (\alpha_c^B - \alpha_l^A) \geq 0 \quad (5)$$

must be met to provide valid solutions, hence extrema. Rewriting the conditions $\varphi > \xi_+$ and $\varphi < \xi_+$ by using the previous expressions for φ and ξ_+ we conclude that only $\varphi > \xi_+$ satisfies condition (5) and hence provides extrema.

However, according with the vertical asymptotic behaviour and the existence of only one crossing point (ξ_+) within the positive domain, we conclude that the extrema are located within $B < 0$. Hence, no extrema can be obtained within the biologically meaningful domains ($A > 0, B > 0$) for neither scenario. In figure 2(b),(c) the two different types of possible behaviour are shown. Furthermore, a similar analysis has been performed for a system without basal transcription and the geometrical features are not affected qualitatively.

Fixed point analysis. Using the previous geometrical approach, we are in the position to reassemble both nullclines within the biological meaningful region. Four possible cases are obtained based on the symmetry of the expressions for nullcline $\dot{A} = 0$ and $\dot{B} = 0$. They are shown in figure 3. For the cases $[\xi_+ > \varphi]_{\dot{A}=0} \wedge [\xi_+ < \varphi]_{\dot{B}=0}$ and $[\xi_+ < \varphi]_{\dot{A}=0} \wedge [\xi_+ > \varphi]_{\dot{B}=0}$ (3(a) and 3(b), respectively), equal geometrical arguments apply. In both cases the nullclines exhibit opposite monotonicities and opposite curvatures within the entire domain due to the absence of extrema and inflexion points. These conditions solely allow for a single crossing, hence monostability. In the case $[\xi_+ < \varphi]_{\dot{A}=0} \wedge [\xi_+ < \varphi]_{\dot{B}=0}$, depicted in figure 3(c), the nullclines exhibit opposite curvature, but equal monotonicities. Again, the absence of extrema and inflection points does not allow for three crossings, however under the special condition of $[\xi_+]_{\dot{A}=0} = [\xi_+]_{\dot{B}=0} = 0$ two crossing point arise. In accordance with expression (4), these conditions can be satisfied, if $4d_i\gamma_i\omega_i^i = 0$ with $i = \{A, B\}$. Since $\gamma_i > 0$ and $d_i > 0$, only ω_i^i can be zero and in this case (for a system without autoloop regulation) the nullclines' expressions now read:

$$\begin{aligned} B &= \frac{\gamma_A - d_A A}{\omega_c^B (d_A A - \gamma_A \alpha_c^B)} \\ A &= \frac{\gamma_B - d_B B}{\omega_c^A (d_B B - \gamma_B \alpha_c^A)}, \end{aligned} \quad (6)$$

where the fixed points can be analytically solved. The solutions are determined by the roots of a polynomial of second degree allowing for two possible fixed points at most. However, the polynomial crosses the vertical axis at $-\gamma_A \gamma_B \omega_c^A \alpha_c^A$ forcing one of the roots to be located within the negative domain. Hence, without autoloops only monostability is possible in monomeric gene circuits.

For the setting $[\xi_+ > \varphi]_{\dot{A}=0} \wedge [\xi_+ > \varphi]_{\dot{B}=0}$ both nullclines show the same type of curvature and monotony. Due to the oblique asymptote, introduced by the autoloop, no analytical constraints prevent the existence of three crossing points. In figure 3(d) we show an example of bistability with monomeric regulation.

In order to determine the impact of the number of autoloops on bistability, we have numerically analyzed the effect of downsizing the system from two to one autoloop ($\omega_i^i = 0, \omega_i^j > 0$). As figure 4 shows, only one autoloop is required to allow bistability. In figure 4(a) the nullclines of a circuit with two autoloops are depicted and

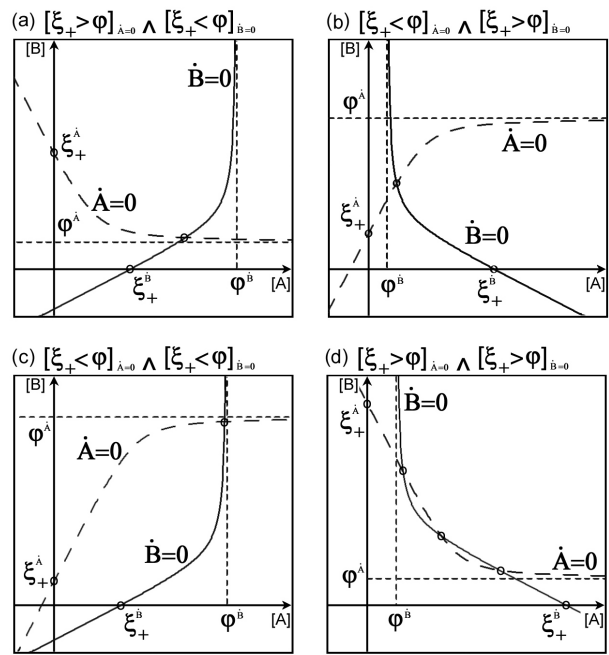


FIG. 3: The four possible scenarios of nullcline combinations. Dashed line corresponds to nullcline $\dot{A} = 0$, solid line to $\dot{B} = 0$, φ^A and φ^B denote the location of the asymptote for $\dot{A} = 0$ and $\dot{B} = 0$, respectively. Due to the symmetry of the nullclines' expressions, the vertical asymptote of $\dot{B} = 0$ corresponds to the horizontal of $\dot{A} = 0$. Analogously, ξ_+^A and ξ_+^B are the crossing points with the axis. (d) The geometrical features of the nullclines allow for two possible cases. Three crossing points (depicted) or a single crossing (not depicted).

three fixed points appear for a given set of parameters. The stability analysis reveals two stable fixed points separated by an unstable one resulting in the corresponding basins of attraction. Figure 4(b) shows a system with a single autoloop. These numerical examples demonstrate that genetic circuits with monomeric regulation are able to exhibit deterministic bistability, whereby only a single autoloop is required to satisfy the necessary geometrical constraints.

Impact of regulation type on monomeric bistability. In the previous sections the type of regulatory interactions, given by α_i^i and α_c^i was handled generally. However, the individual regulatory interactions, i.e. activation or inhibition, introduces additional constraints for the emergence of bistability. Applying some algebra to condition $\varphi < \xi_+$ (bistability), we obtain an equivalent expression as in (5) with the opposite inequality. Focusing on the type of regulation, it can be rewritten as

$$\alpha_i^A > \alpha_c^B - \frac{(1 - \alpha_c^B)d_A}{\alpha_c^B \gamma_A \omega_i^A}. \quad (7)$$

This leads us to two different instances: (a) if $\alpha_c^B > 1$, then $\alpha_i^A > \alpha_c^B$ and (b) if $\alpha_c^B < 1$, then $\alpha_i^A > \alpha_c^B \vee \alpha_i^A < \alpha_c^B$. As a consequence systems with inhibitory regulation

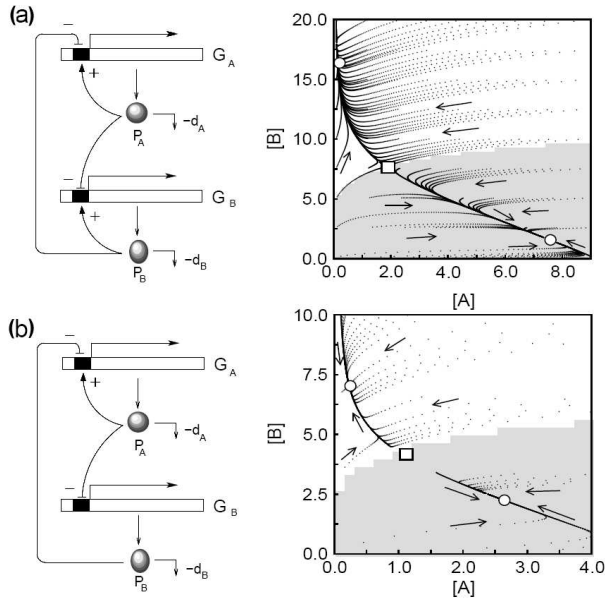


FIG. 4: Numerical simulations and stability analysis of systems with (a) two and (b) one autoloop. Circle denotes a stable, square an unstable fixed point. The basins of attraction are shown in grey and white. The following sets of parameters have been used: (a) $\gamma_A = 1$, $d_A = 1$, $\alpha_l^A = 10$, $\omega_l^A = 1$, $\omega_c^B = 1$, $\alpha_c^B = 0$, $\gamma_B = 1.1$, $d_B = 0.1$, $\alpha_l^B = 2.1$, $\omega_l^B = 0.1$, $\omega_c^A = 1.1$, $\alpha_c^A = 0$ and (b) $\gamma_A = 5$, $d_A = 8$, $\alpha_l^A = 9$, $\omega_l^A = 1$, $\omega_c^B = 1$, $\alpha_c^B = 0$, $\gamma_B = 8.5$, $d_B = 1$, $\alpha_l^B = 0$, $\omega_l^B = 0$, $\omega_c^A = 1$, $\alpha_c^A = 0$

in the autoloop and activatory cross-regulation can not exhibit bistability. In all the other cases no geometric impediments are present.

Discussion. To summarize, a general, analytic set of conditions for bistability in simple two-element genetic circuits has been derived for monomeric regulation. Although previous work suggested that such kind of mechanism would be unlikely to be observed, here a simple geometric argument reveals that wide parameter spaces allow monomeric regulation to generate multiple stable states. These results permit to predict the expected scenarios where a reliable switch could be obtained. Current efforts in engineering cellular systems [24–26] would benefit from our general analysis. In this context, although dimerization seems to be a widespread mechanism in GRNs, our study indicates that potential scenarios for monomeric regulation could be easily achieved through the appropriate engineered components. Finally, further work should explore how noise can act on these type of dynamical systems. In eucaryotic cells, dimerization has been shown to provide a source of noise reduction at least at the level of simple GRNs [27]. Future studies should see how our monomeric circuits are affected by noise and what types of limitations and advantages can be obtained.

We thank the members of the CSL for useful discussions. This work has been supported by a EU grant CELLCOMPUT, the James McDonnell Foundation and by the Santa Fe Institute.

-
- *
- [1] Laurent, M. and Kellershohn, N. (1999) *Trends Biochem. Sci.* **24**, 418.
 - [2] Ferrell, J. E. and Machleder, E. M. (1998) *Science* **280**, 895.
 - [3] Chickarmane et al. (2006) *PLOS Comput. Biol.* **2**, e123.
 - [4] Pomereaney, J. R. et al. (2003) *Nature Cell. Biol.* **5**, 346.
 - [5] Dubnau, D., Losick, R. (2006) *Molecular Microbiology* **61**(3), 564-572.
 - [6] Oppenheim, A.B., Kobiler, O., Stavans, J., Court, D.L., Adhya, S. (2005) *Annu. Rev. Genet.* **39**, 409-429.
 - [7] Tian, T., Burrage, K. (2004) *J. Theor. Biol.* **227**, 229-237.
 - [8] Becksei, A., Seraphin, B. and Serrano, L. (2001) *EMBO J.* **20**, 2528.
 - [9] Hasty, J., McMillen, D. and Collins, J. J. (2002) *Nature* **420**, 224.
 - [10] Elowitz, M.B., Leibler, S. (2000) *Nature* **403**, 335 - 338.
 - [11] Hasty, J., Dolnik, M. Rottschäfer, V., Collins, J.J. (2002) *Phys. Rev. Lett.* **84**, 148101.
 - [12] Gardner, T.S., Cantor, C.R., Collins, J.J. (2000) *Nature* **403**, 339 - 342.
 - [13] Lipshtat, A., Loinger, A., Balaban, N.Q., Biham, O. (2006) *Phys. Rev. Lett.* **96**, 188101.
 - [14] Tian, T., Burrage, K. (2006) *Proc. Natl. Acad. Sci. USA* **103**, 8372-8377.
 - [15] Santillán, M., Mackey, M.C. (2005) *Biophys. J.* **86**, 75-84.
 - [16] Hasty, J., Pradlines, J., Collins, J.J. (2000) *Proc. Natl. Acad. Sci. USA* **97**, 2075-2080.
 - [17] Hasty, J., Isaacs, F. (2001) *Chaos*, **11**, 207-220.
 - [18] Warren, P.B., ten Wolde, P.R. (2004) *Phys. Rev. Lett.* **92**, 128101.
 - [19] Widder, S., Schicho, P., Schuster, P. (2007) *J. Theor. Biol.* **246**, 394-419.
 - [20] Loinger, A., Lipshtat, A., Balaban, N.Q., Biham, O. (2007) *Phys. Rev. E* **75**, 021904. *Annu. Rev. Genet.* **39**, 409-429.
 - [21] Tyson, J. J., Chen, K. C., Novak, B. (2003) *Curr. Opin. Cell. Biol.* **15**, 221-231.
 - [22] Warren, P. B., ten Wolde, P. R. (2005) *J. Phys. Chem. B.* **109**, 6812-6823.
 - [23] Walczak, A. M., Sasai, M., Wolynes, P. G. (2005) *Biophys. J.* **88**, 828-850.
 - [24] Ferrell, J. E. (2002) *Curr. Opin. Chem. Biol.* **6**, 140.
 - [25] McDaniel, R. and Weiss, R. (2005) *Curr. Opin. Biotech.* **16**, 476.
 - [26] Solé, R. V., Munteanu, A., Rodriguez-Caso, C. and Marcia, J. (2007) *Phil. Trans. R. Soc. London B* **362**, 1821.
 - [27] Bundschuh, R., Hayot, F. and Jayaprakash, C. (2003) *J. Theor. Biol.* **220**, 261.